Supporting Information

Broadband Waveguide Electro-Optic Comb Enabled by Mode Circulation

Aoyun Gao[1], Jiaxuan Gan[1], Mingyu Zhu[1], Weihan Wang[1], Fei Huang[1], Liu Liu[1], Weike Zhao[1,*] and Daoxin Dai[1,*]

[1]*State Key Laboratory for Extreme Photonics and Instrumentation, College of Optical Science and Engineering, Zhejiang University, Hangzhou 310058, China.*

*Corresponding author: dxdai@zju.edu.cn, wkzhao@zju.edu.cn

Keywords: Lithium niobate, Electro-optical modulation, comb, mode (de)multiplexer, Multi-pass

S1: Passive element design

Mode (De)multiplexers: To address the mode hybridization problem of the anisotropic LNOI waveguide, the mode (de)multiplexer (MUX) is designed with Z-propagation waveguides. The MUX consists of three cascaded adiabatic directional couplers (ADCs), each designed to selectively (de)multiplex one of the higher-order modes (TE_1, TE_2, and TE_3). The general structure of a single ADC unit is shown in Supplementary Figure S1(a). It consists of two tapered waveguides: an access waveguide (tapering from w_{a1} to w_{a2}) and a bus waveguide (tapering from w_{b1} to w_{b2}), separated by a coupling gap g_c over a coupling length L_c. To ensure selective conversion for each mode, the geometric parameters for ADC1 (TE_1), ADC2 (TE_2), and ADC3 (TE_3) were independently optimized. The final design parameters are summarized in Supplementary Table 1. The simulated transmission spectra for each of the three optimized ADCs are shown in Supplementary Figure S1(b)~(d). These simulations confirm that the design achieves an ultra-low excess loss (EL < 0.1 dB) and low inter-modal crosstalk (crosstalk < -22 dB) across a broad bandwidth of 1450–1650 nm for all three mode-channels.

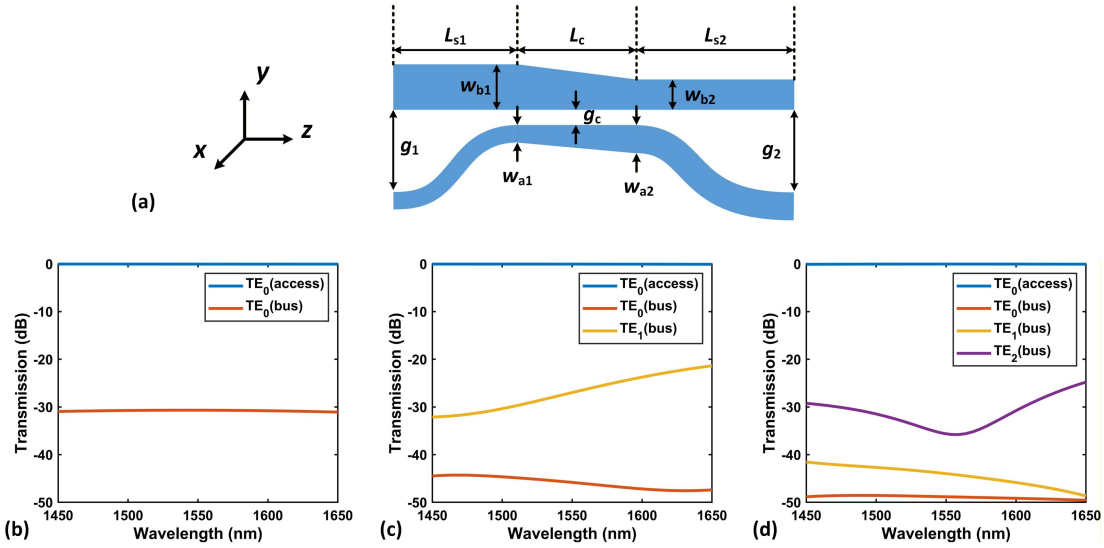

Figure S1. Design of the mode MUX. (a) Schematic of a single adiabatic directional coupler (ADC) unit. Calculated transmissions of the designed ADCs for the (b)TE_1, (c)TE_2, (d)TE_3 modes.

Supplementary Table 1. Key parameters of the designed ADCs for three higher-order modes.

Parameters [μm]	w_{b1}	w_{b2}	w_{a1}	w_{a2}	L_c	g_c
TE_1	1.45	0.9	0.15	0.45	100	0.35
TE_2	2.45	1.75	0.15	0.45	100	0.35
TE_3	3.45	2.9	0.15	0.45	100	0.35

Multimode bending waveguide: The width of the multimode bending waveguide (MBW) and multimode bus waveguide is designed with a width of 4 μm to support four optical modes as well as avoid the mode hybridization width of the Y-propagation waveguide. The simulation results demonstrate that the MBW (with a R_{max}=1500 and R_{min}=90 μm) achieves low excess loss (EL < 0.1 dB) and low crosstalk (crosstalk < -18 dB) across a broadband wavelength range of 1500-1600 nm for all four optical modes, as detailed in Supplementary Figure S2.

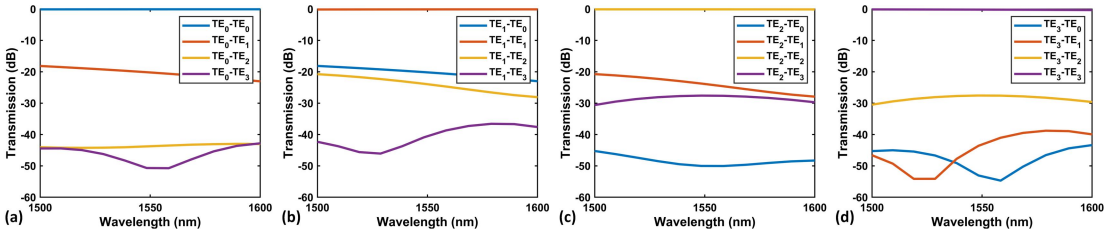

Figure S2. Calculated transmissions of the designed 90° MBW. For the (a) TE_0, (b) TE_1, (c) TE_2, (d) TE_3 modes.

Waveguide crossing: The schematic of the MMI-based waveguide crossing is shown in Supplementary Figure S3(a). To optimize the self-imaging position and achieve minimal loss for both intersecting paths, the lengths of the central multimode sections are designed as L_1 = 31 μm for the Z-propagation axis and L_2 = 35 μm for the Y-propagation axis. Connected to this central region, the input/output single-mode waveguides (w_1 = 2 μm) are adiabatically widened to a multimode width of w_2 = 4 μm over a taper length of L_3 = 7 μm. This design achieves a simulated insertion loss of less than 0.05 dB for both propagation axes across the 1500–1600 nm wavelength range, as shown in Supplementary Figure S3(b).

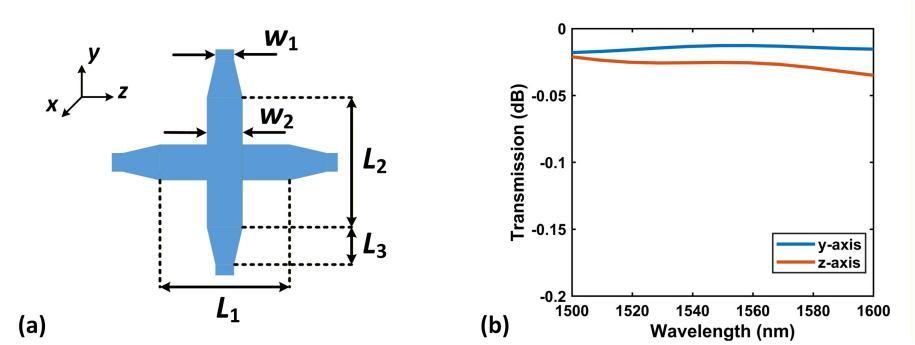

Figure S3. Design of the waveguide crossing. (a) Schematic illustration of the waveguide crossing, (b) calculated transmissions of the designed waveguide crossing for the TE_0 mode.

Delay line design:

Supplementary Table 2. The waveguide path length and the corresponding effective round-trip time for each loop.

Waveguide loop	L_t (mm)	$T/\Delta T_{25GHz}$
Loop #1 (TE_0)	26.348	5
Loop #2 (TE_1)	26.199	5
Loop #3 (TE_2)	25.984	5
Loop #4 (TE_3)	28.341	5.5
Loop #5 (TE_0)	26.348	5
Loop #6 (TE_1)	26.199	5
Loop #7 (TE_2)	25.984	5
Total	185.403	35.5

S2: Calculation of Modulation Response

The overall modulation frequency response, $m[\omega]$, of the traveling-wave modulator is a critical parameter that determines the electro-optic (E-O) bandwidth. It can be expressed as a function of the microwave and optical properties of the device. Assuming both the source and load impedances are 50 Ω, the modulation response in decibels is given by:

$$m[\omega] = 20\log_{10}\left\{\frac{2Z_{in}}{Z_{in}+50}\cdot\frac{(50+Z_0)\cdot F_+ + (50-Z_0)\cdot F_-}{(50+Z_0)\cdot e^{\gamma_m L} + (50-Z_0)\cdot e^{-\gamma_m L}}\right\}$$

where ω is the angular frequency of the RF signal, Z_{in} is the impedance seen at the input of the electrode, L is the length of the modulation region, and γ_m is the RF propagation constant. One has

$$Z_{in} = Z_0\frac{50 + Z_0\cdot\tanh(\gamma_m L)}{Z_0 + 50\cdot\tanh(\gamma_m L)}$$

$$\gamma_m = \alpha_m + j\frac{\omega}{c_0}n_m$$

$$F_\pm = \frac{1 - e^{\pm\gamma_m L - j\frac{\omega}{c_0}n_g L}}{\pm\gamma_m L - j\frac{\omega}{c_0}n_g L}$$

Here, n_g represents the group refractive index of the specific optical mode, denoted as $n_{g\text{-TE0}}$~$n_{g\text{-TE3}}$ for the respective modes. Figure 3 (f) of the main text shows the calculated modulation response $m[\omega]$ for all optical modes.

S3: E-O comb simulation and measurement

The present mode circulating E-O comb can be modeled as a series of cascaded phase modulators. When a CW input $E_{in}(t) = E_0 e^{i\omega ct}$ is modulated by a sinusoidal RF signal, the output field is:

$$E_{out}(t) = E_0 e^{i\omega_c t} e^{i\beta\cos(\omega_{RF}t)}$$

where $\beta = \pi\cdot V_m/V_\pi$ is the modulation index, and V_m represents the peak voltage of the modulation radio frequency signal, and V_π is the half-wave voltage of the phase modulator. In the frequency domain, this field expands via a Jacobi-Anger expansion:

$$E(\omega) \propto \sum_{n=-\infty}^{+\infty} J_n(\beta)\delta\big(\omega - (\omega_c + n\omega_{RF})\big)$$

The power of the n-th comb line is therefore proportional to $|J_n(\beta)|^2$, and the comb spectral envelope is inherently non-flat, as the simulation results illustrated in Supplementary Figure S4(a) for present E-O comb with one (β = 5.4 π), two (β = 9.6 π), three (β = 13.8 π), and four (β = 17.2 π) mode-channels.

To achieve a flat-top spectrum, a time-to-frequency mapping method is adopted by cascading an intensity modulator (IM) and a phase modulator (PM). The IM first carves the CW laser into a temporal pulse train. The output field after the IM can be expressed as:

$$E_{IM}(t) = E_{in}(t) \cdot \cos\left(\frac{\pi}{2}\frac{V_{IM}(t) + V_{DC}}{V_{\pi,IM}}\right)$$

where $V_{IM}(t) = V_{RF,IM}\sin(\omega_{RF}t)$ is the RF drive signal, V_{DC} is the DC bias voltage, and $V_{\pi,IM}$ is the half-wave voltage of the IM. By optimizing V_{DC} and $V_{RF,IM}$ to exploit the nonlinear transfer function of the IM, a periodic train of flat-top (rectangular-like) temporal pulses is generated.

This pulse train is then synchronized with the PM, which imparts a strong, time-varying phase shift $\Phi_{PM}(t)=\beta_{PM}\cos(\omega_{RF}t)$. By aligning the temporal pulse to the crest (or trough) of the PM's RF drive signal, the sinusoidal phase modulation can be approximated by a quadratic function (Taylor expansion):

$$\phi_{PM}(t) \approx \phi_0 - \frac{1}{2}\beta_{PM}(\omega_{RF}t)^2 = \phi_0 - C \cdot t^2$$

where C is the chirp constant. This quadratic phase acts as a "time lens," performing a temporal Fourier transform that maps the flat-top temporal envelope shaped by the IM to the desired flat-top spectral envelope $\widetilde{E}(\omega)$.

Supplementary Figure S4(b) illustrates the simulated spectrum of the standalone four-mode-channel E-O comb (β = 11 π), which exhibits a typical Bessel-like distribution. In contrast, Supplementary Figure S4(c) demonstrates the substantially improved spectral flatness achieved by connecting an IM to this comb. In this simulation, the IM is biased at a specific point (e.g., $V_{DC} \approx 0.35V_{\pi,IM}$) and driven by a large amplitude signal to clip the sinusoidal peak, creating the necessary flat-top temporal profile for effective mapping.

The experimental setup for flat-top comb generation is depicted in Supplementary Figure S5. The light from a tunable laser (TL) was first modulated by an external commercial IM to generate the periodic temporal pulses. Subsequently, this pulse train was coupled into our four-mode-channel E-O comb chip. The RF signal from a clock source was split into two paths by a power divider and amplified to drive the IM and our PM, respectively. A tunable RF phase shifter was used to precisely control the relative phase between these two RF paths,

ensuring synchronization between the peak of the temporal pulse and the imparted phase chirp. By co-optimizing the DC bias of the IM (2.6 V), the RF driving powers (19 dBm to the IM and 28 dBm to the PM), and the relative phase between the two modulators, we successfully generated a broadband, flat-top optical frequency comb.

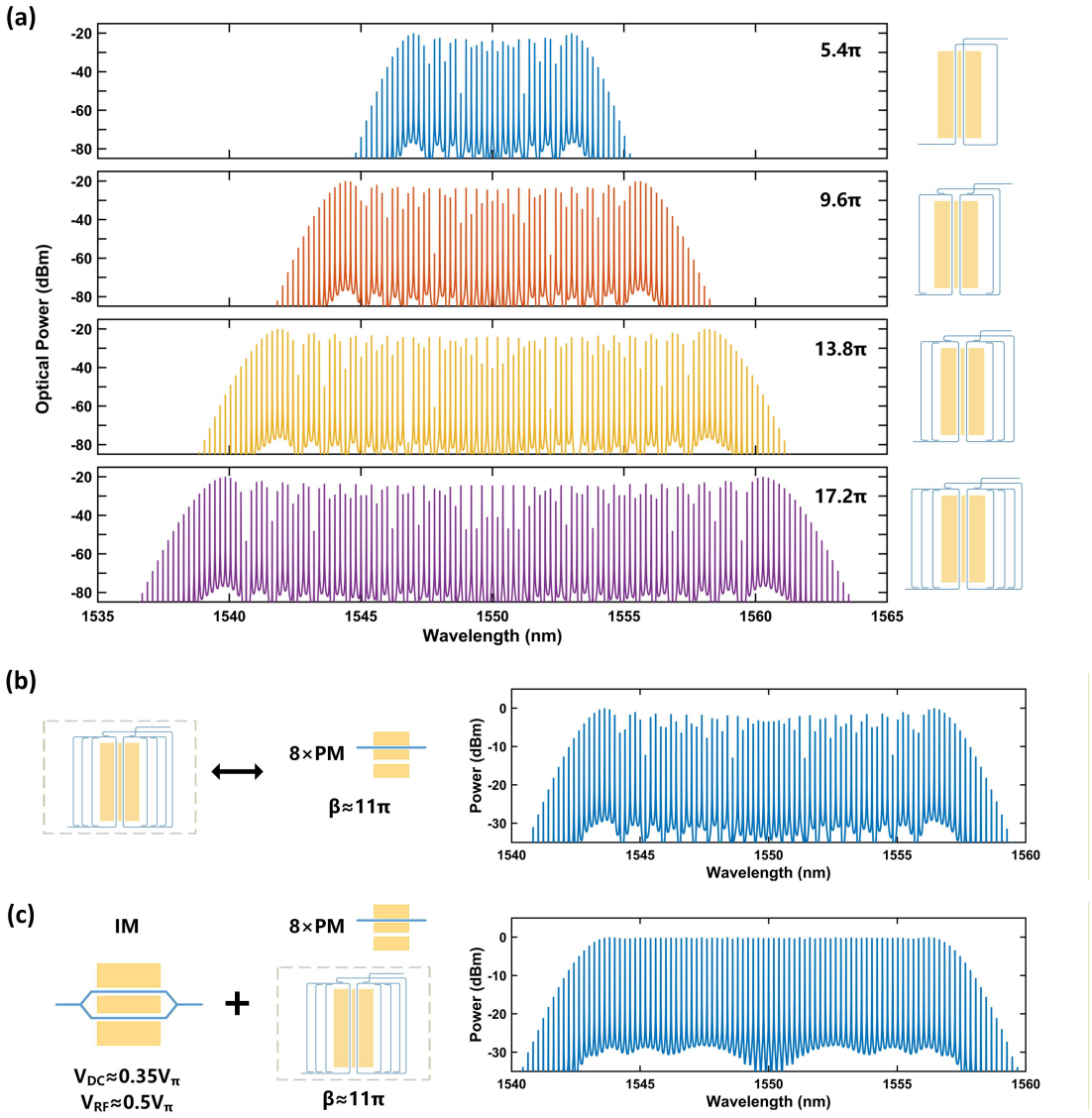

Figure S4. Principle and simulation of flat-top comb generation. (a) Simulated E-O comb spectra for the one-, two-, three-, and four-mode-channel E-O comb, illustrating the characteristic non-flat spectral envelope. Spectrum comparison between (b) the standalone four-mode-channel E-O comb (β = 11 π), and (c) the flat-top comb constructed by connecting an IM to this four-mode-channel E-O comb.

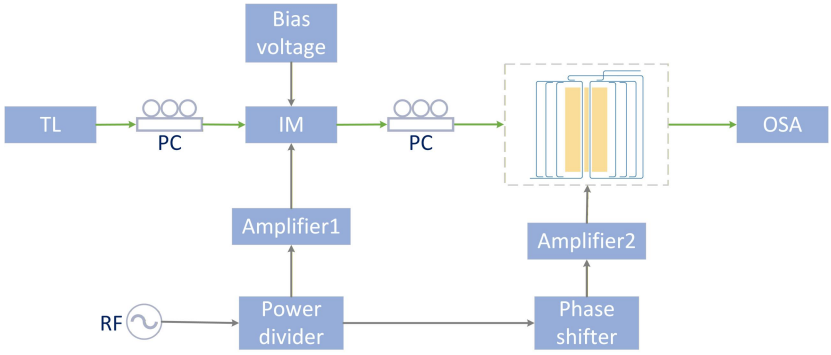

Figure S5. Experimental setup for generating a flat-top comb. TL: Tunable Laser; PC: Polarization Controller; IM: Intensity Modulator; RF: Radio Frequency source; PM: Phase Modulator (the 4-pass mode-circulating chip); OSA: Optical Spectrum Analyzer.

S4: Spectral measurement:

The method relies on performing two distinct heterodyne measurements between the tunable E-O comb and the signal under test (with frequency f_s). This process yields two intermediate frequencies, f_{m1} and f_{m2} (both less than half of the repetition rate). For the first measurement, the E-O comb is generated with a pump laser frequency of f_p and a repetition rate of f_{r1}. For the second measurement, the pump laser frequency is shifted by f_{ps} (where $f_{ps} > 0$) to $f_p + f_{ps}$, and the repetition rate is changed to f_{r2} (where $f_{r2} > f_{r1}$). The corresponding two comb spectra are shown in Figure 6(b) of the main text. This process can be described by the following equations:

$$\begin{cases} f_{m1} = |f_p + n \cdot f_{r1} - f_s| \\ f_{m2} = |f_p + f_{ps} + n \cdot f_{r2} - f_s| \end{cases}$$

where n is the unknown integer mode number of the comb line closest to the signal. By solving this system of equations, both n and the unknown signal frequency f_s can be determined unambiguously. In our experiment, we set the initial pump frequency f_p = 193.548 THz (corresponding to λ = 1550 nm), the pump frequency shift f_{ps} = 0.125 GHz, and the repetition rates f_{r1} = 24.54 GHz and f_{r2} = 24.64 GHz.